ELSEVIER

Journal of Nuclear Materials 253 (1998) 1–9

journal of nuclear materials

Section 1. Mechanical properties of unirradiated and irradiated SiC composites

The mechanical behavior of a Nicalon/SiC composite at room temperature and 1000°C

N. Miriyala [a,1], P.K. Liaw [a], C.J. McHargue [a], L.L. Snead [b,*]

[a] *Department of Materials Science and Engineering, The University of Tennessee, Knoxville, TN 37996, USA*
[b] *Metals and Ceramics Division, Oak Ridge National Laboratory, PO Box 2008, Oak Ridge, TN 37831, USA*

Abstract

The effects of fabric orientation on the mechanical behavior of a Nicalon/SiC composite were investigated by performing flexure tests at room temperature in air, and at 1000°C in an argon environment. The specimen configurations were designated as edge-on and transverse, depending on whether the load was applied parallel or normal to the fabric plies, respectively. The monotonic and fatigue behavior of the material was not noticeably affected by fabric orientation, at both room and elevated temperatures. The interlaminar pores in the material appeared to have acted as stress concentration sites. The cracks initiated from these sites linked up the interlaminar pores, resulting in specimen severance under monotonic and fatigue loadings, in both edge-on and transverse orientations. © 1998 Elsevier Science B.V.

1. Introduction

The potential advantages of using low atomic number (Z) ceramics, such as silicon carbide (SiC), for structural applications in fusion reactors include: (a) improved plant conversion efficiencies due to higher operating temperatures, (b) reduction in the high Z impurities transported into the plasma from the first wall, and (c) less severe waste generation due to neutron activation [1–3].

Monolithic, or unreinforced, ceramics are undesirable from a design point of view because they are intrinsically brittle and fail in a catastrophic manner. However, significant increases in the material toughness can be obtained by reinforcing the brittle-ceramic matrices with continuous fibers. Toughness by fiber reinforcement relies upon a weak bond between the fiber and the matrix, obtained by using fiber-coatings of low modulus materials such as carbon and boron nitride [4,5]. These materials are known as continuous fiber-reinforced ceramic-matrix composites (CFCCs).

The most widely used method in the manufacture of bi-directionally (2D) reinforced CFCCs is to infiltrate a woven or braided fiber-fabric preform using liquid or vapor phase infiltration techniques [6,7]. The composite laminates may suffer from interlaminar weakness, which usually manifests in the form of delamination or interlaminar cracks [4,5,8,9]. Hence, it is expected that the mechanical behavior of 2D CFCCs, under monotonic and fatigue loadings, can be affected by the orientation of the fabric plies to the loading direction. Accordingly, it was the objective of the present study to systematically investigate the effects of fabric orientation on the monotonic and fatigue behavior of a commercially available CFCC, namely a 2D braided Nicalon fiber-fabric reinforced SiC matrix composite manufactured by a chemical vapor infiltration (CVI) process (Nicalon is the trade name for the Si–C–O fibers manufactured by Nippon Carbon Company, Japan with a chemical composition, in weight percent, of 59 Si, 31 C and 10 O).

2. Experimental details

2.1. Material

The 2D braided Nicalon/SiC composite used in the present study was fabricated by E.I. du Pont de Nemours

* Corresponding author. Fax: +1-423 576 8424; e-mail: z2n@ornl.gov.
[1] Present Address: Solar Turbines Inc., San Diego, CA 92186-5376, USA.

PII S0022-3115(97)00341-3

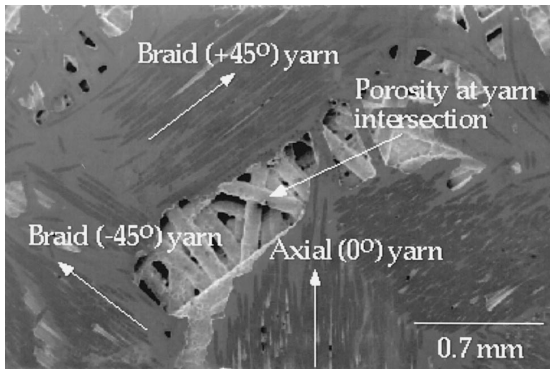

Fig. 1. Planar view of the Nicalon/SiC composite microstructure.

and Company, Newark, DE, using an isothermal chemical vapor infiltration (ICVI) process. In the ICVI method, a fabric preform is first given a thin coating of carbon to obtain a weak interface between the fiber and the matrix. Two reactant gases, methyltrichlorosilane (CH_3SiCl_3) and hydrogen, are then introduced into the preform at 1,100 to 1,200°C. The CH_3SiCl_3 gas decomposes into SiC and HCl ($CH_3SiCl_3 \rightarrow SiC + 3HCl$), and the SiC deposits as a solid coating onto the fiber surfaces. This coating constitutes the matrix in the composite. The process continues until reduced permeability of the densified composite prevents a sufficient flow of reactant gases into the preform. Consequently, the composites contain significant amounts of porosity [7].

A planar view of the Nicalon/SiC composite microstructure is presented in Fig. 1. The axial (0°) and braid ($\pm 45°$) yarns are clearly identified in Fig. 1. The average width of the braid yarns is approximately 0.001 m. It can be seen from Fig. 1 that pores are present in the material at the yarn intersections. Porosity was also observed between the laminae, and the interlaminar pores were of different shapes and sizes [10]. The size of the interlaminar pores varied from 0.0001 to 0.001 m [10]. The nominal fiber volume fraction in the composite was approximately 0.4.

2.2. Specimen types and fabrication

The as-received material was in the form of a plate, approximately 0.205 m long, 0.140 m wide, and 0.0021 to 0.0024 m thick. The composite plate surfaces were flat-ground to obtain specimens of uniform thickness. A majority of the specimens fabricated were 0.050 m long with a 0.002 m × 0.002 m cross-section. These specimens were used to perform monotonic and fatigue tests on the Nicalon/SiC composite. The square cross-section was chosen so that an objective assessment of fabric orientation effects on the monotonic and fatigue behavior of the material could be made. In addition, to study the effect of loading span on the ultimate flexural strength (UFS) values, some specimens of 0.090 m in length, but of the same cross-section, were also machined (the choice of 0.090 m for the specimen length was influenced by the space available in the furnace used during the elevated-temperature flexure testing). Further, to elucidate the effect of specimen size on the monotonic behavior, some wider (0.006 m) specimens of 0.050 m and 0.090 m length were also prepared.

2.3. Mechanical tests

The mechanical tests were performed on a servohydraulic load-frame (Model 810, MTS Systems Corporation, Minneapolis, MN) equipped with a graphite-element resistance-heating furnace. The load frame was interfaced to an IBM personal computer through a controller (Interlaken Series 3200, Interlaken Technology Corporation, Eden Prairie, MN). A universal testing program (UTP-III), developed by the Interlaken Technology Corporation, was used to conduct all the mechanical tests and record the data in a digital form.

The monotonic tests were performed under four-point bend loading, using the general guidelines of ASTM Standard C 1341 [11]. The flexure tests at room temperature (RT) were performed in air, and those at 1000°C were conducted in an argon environment. A semi-articulating bend fixture made of SiC was used for this purpose. During the high-temperature tests, the temperature near the samples was maintained at 1000 ± 2°C. The loading and supporting spans were 0.020 m and 0.040 m, respectively, during the flexure testing of the 0.050 m long specimens. Likewise, the loading pins were 0.040 m apart and the supporting pins were at a distance of 0.080 m from one another during the bend testing of the 0.090 m long specimens. The tests were conducted under displacement control at a crosshead movement rate of 0.0005 m/min. A SiC rod in contact with the center of the tensile (bottom) surface of the flexure specimen was used to measure the midspan deflection using a displacement gage (Model 632.70-01, MTS Systems Corporation, Minneapolis, MN).

The fatigue tests at RT and 1000°C were performed using 0.050 m long specimens. A stress-life (S–N) approach was used to conduct the cyclic-fatigue tests under load control, using a sinusoidal wave form. The cyclic frequency was 0.5 Hz up to the first 1000 cycles, and then gradually increased to 5 Hz and maintained at that frequency until the completion of the tests. A load ratio (minimum load/maximum load) of 0.1 was used in all the fatigue tests. The fatigue runout was set at one million (10^6) cycles, which corresponded to approximately 56 h of testing.

During the monotonic and fatigue tests, the loads applied to the specimens were either parallel or perpendicular to the fabric plies. Accordingly, the specimen configurations were referred to as edge-on and transverse, depend-

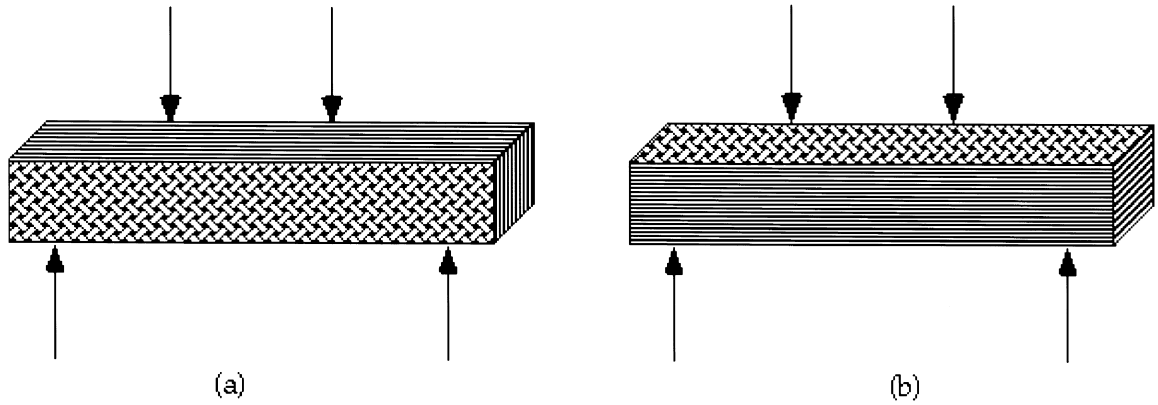

Fig. 2. Geometries for flexure-testing laminate composites: (a) edge-on and (b) transverse.

ing on whether the load was parallel or normal to the fabric plies, respectively (Fig. 2).

3. Results

3.1. Stress–strain behavior

Flexural stress–strain curves were obtained for the Nicalon/SiC composite at room temperature (RT) in air, and at 1000°C in an argon atmosphere. The flexural stress (σ) and strain (ε) values were calculated from the following equations given in the ASTM Standard C 1341 [11]:

$$\sigma = \frac{3PL}{4bh^2} \tag{1}$$

and

$$\varepsilon = \frac{4.36\delta h}{L^2}, \tag{2}$$

where σ is the maximum stress in the outer fibers at a given load (P), L is supporting span, b is the specimen width, h is the thickness, ε is the maximum strain in the outer fibers at a given load, and δ is the midspan deflection.

It is important to note that Eq. (1) does not consider the shift of the neutral axis to the compression side of the specimen, which takes place once cracking occurs on the tensile side of the beam. Since the strength of ceramics, in general, is higher in compression than in tension, neglecting the shift of the neutral axis can result in UFS values that are significantly higher than the ultimate tensile strength (UTS) of the material [12,13]. However, simple equations to calculate the UFS from the maximum load in a flexure test, which take into account neutral axis shift and/or the propagation of interlaminar/delamination cracks, have yet to be developed. Hence, Eq. (1) was used to calculate the stress values in this investigation as a consistent basis to study the fabric orientation effects on the monotonic and fatigue behavior of the Nicalon/SiC composite.

Representative stress–strain curves for the 0.050 m × 0.002 m × 0.002 m specimens tested in flexure at RT are shown in Fig. 3. It is apparent from Fig. 3 that the stress–strain curves are non-linear in both edge-on and transverse orientations. The stress at which the stress–strain curves deviate from linearity (the proportional limit, σ_{pl}) was approximately 120 MPa in both orientations. There was a large scatter in the UFS data from all the samples tested. The average UFS values for 10 specimens each in the edge-on and transverse orientations were 234 ± 18 MPa and 241 ± 22 MPa, respectively. The scatter in the UFS data may be attributed to the variations in the statistical distribution of flaws, fiber volume fraction, pore size and content from sample to sample. In addition, the fiber and the matrix materials may also have a statistical distribution of strengths [14–17]. Of these, only the estimation of porosity content of the samples is simple and practical. The percentage porosity in a sample is related to the bulk

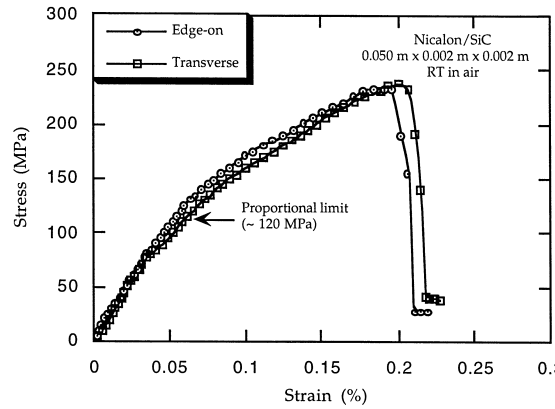

Fig. 3. Flexural stress–strain curves for the 0.050 m × 0.002 m × 0.002 m Nicalon/SiC specimens in the edge-on and transverse orientations at room temperature in air.

density of the specimen, and the theoretical density of the material, by

$$\%\text{porosity} = (1 - \text{bulk density}/\text{theoretical density}) \times 100. \quad (3)$$

The bulk density of the samples was calculated from their weight and dimensions. The theoretical density of the Nicalon/SiC composite was taken to be 2960 kg/m^3 [18]. The porosity content of the specimens used in the monotonic and fatigue tests varied from 11 to 24%.

The stress–strain curves and the UFS data for the 0.050 m × 0.002 m × 0.002 m specimens at 1000°C were similar to those at RT. In both orientations, the σ_{pl} was observed at around 120 MPa. The average UFS values for 10 specimens each in the edge-on and transverse orientations were 245 ± 27 MPa and 250 ± 23 MPa, respectively. From the UFS data for the 0.050 m × 0.002 m × 0.002 m specimens, it was apparent that the monotonic behavior of the Nicalon/SiC composite was unaffected by the fabric orientation and the test temperature.

The UFS data for the 0.090 m × 0.002 m × 0.002 m specimens was analogous to that for the 0.050 m × 0.002 m × 0.002 m specimens at RT and 1000°C. Also, the stress–strain curves at room and elevated temperatures were similar for the 0.090 m × 0.002 m × 0.002 m specimens. At RT, the average UFS values for five specimens each in the edge-on and transverse orientations were 247 ± 18 MPa and 243 ± 30 MPa, respectively. The corresponding values at 1000°C were 264 ± 33 MPa and 269 ± 25 MPa. In both orientations, and at both temperatures, the σ_{pl} values were comparable (~ 120 MPa). It is evident that, for the 0.002 m × 0.002 m cross-sectioned specimens, an increase in the specimen length from 0.050 m to 0.090 m (doubling the loading span) did not discernibly influence the UFS values, either in the edge-on or the transverse orientations, at both test temperatures.

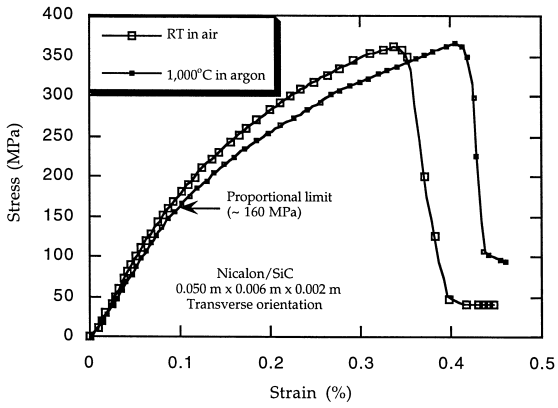

Fig. 4. Flexural stress–strain curves for the 0.050 m × 0.006 m × 0.002 m Nicalon/SiC specimens in the transverse orientation at RT in air, and at 1000°C in argon.

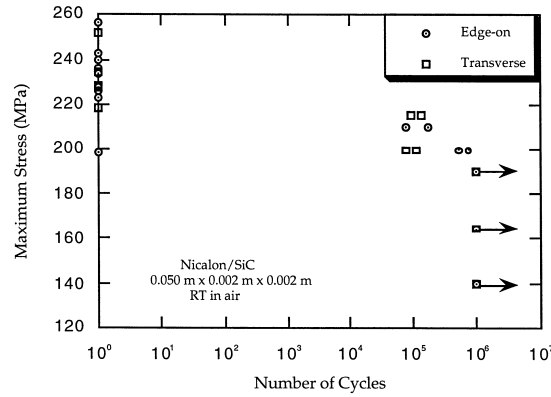

Fig. 5. $S-N$ curves for the Nicalon/SiC composite at room temperature in air.

When the specimen width, however, was changed from 0.002 m to 0.006 m, there was a significant increase in the UFS and σ_{pl} values. These specimens were tested only in the transverse orientation. For the 0.050 m × 0.006 m × 0.002 m size specimens, the stress–strain curves were similar at RT and 1000°C (Fig. 4). Also, the σ_{pl} was about 160 MPa at both temperatures. The average UFS values for 8 specimens each of 0.050 m × 0.006 m × 0.002 m at RT and 1000°C were 358 ± 24 MPa and 380 ± 19 MPa, respectively.

For the specimens with cross-sections of 6 mm × 2 mm, a change in the specimen length from 0.050 mm to 0.090 mm (doubling the loading span) did not remarkably affect the stress–strain behavior. For the 0.090 m × 0.002 m × 0.002 m size specimens, the average UFS value for 6 specimens each at RT and 1000°C were 416 ± 45 MPa and 351 ± 20 MPa, respectively. The stress–strain curves at the room and elevated temperatures were non-linear, and the σ_{pl} was observed at about 150 MPa.

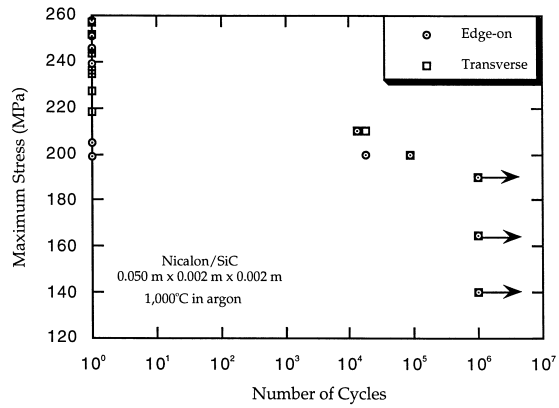

Fig. 6. $S-N$ curves for the Nicalon/SiC composite at 1000°C in argon.

3.2. S–N behavior

The number of cycles to failure at different maximum stress (σ_{max}) levels, in both edge-on and transverse orientations, were determined using the 0.050 m × 0.002 m × 0.002 m size specimens. The *S–N* data for the Nicalon/SiC composite at RT and 1000°C are presented in Figs. 5 and 6, respectively. At room and elevated temperatures, the fatigue limit (the stress at which the specimens survived one million load cycles) was 190 MPa (about 80% of the average UFS) in both orientations. A comparison of Figs. 5 and 6 reveals that the *S–N* data at RT and 1000°C are almost identical. Apparently, neither the fabric orientation nor the test temperature noticeably affected the *S–N* behavior of the Nicalon/SiC composite.

During the cyclic-fatigue tests, the load and midspan deflection values were recorded at periodic intervals. The slope of the linear portion in the load versus midspan deflection traces at a point during the fatigue test was normalized with respect to the slope for the first cycle. The normalized slope was considered to be the 'effective modulus' in the present study. It should be noted here that the calculation of the elastic modulus for a ceramic specimen in flexure is cumbersome, due to the differences in the elastic moduli in tension and compression. Also, the neutral axis shifts towards the compression side, once cracking occurs on the tensile surface of the specimen [12,13]. Therefore, the 'effective modulus' values were used in this investigation only to *qualitatively* monitor progressive damage in the material due to fatigue loading.

For the Nicalon/SiC specimens tested in fatigue at RT and 1000°C, the effective modulus values dropped after the first load cycle in both orientations. The modulus values decreased rapidly in the first 10 load cycles, and then continued to drop steadily up to about 1000 cycles. Beyond 1000 cycles, there was only a marginal reduction in the effective modulus values in both orientations. The trends in effective modulus with number of cycles were similar for the samples tested in both orientations, and at room and elevated temperatures. The trends in effective modulus for the specimens fatigue tested at 1000°C in the transverse orientation are presented in Fig. 7.

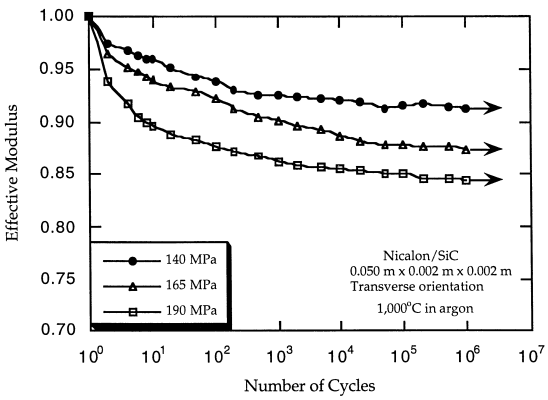

Fig. 7. The reduction in effective modulus due to fatigue in the transverse orientation of the Nicalon/SiC composite at 1000°C in argon.

4. Discussion

4.1. Damage mechanisms

The failure of the Nicalon/SiC samples under monotonic and fatigue loadings was characterized by specimen separation into two pieces. The appearances of the fracture surfaces were similar for the specimens tested in either edge-on or transverse orientations, at room and elevated temperatures. Fiber pullout was observed in all the specimens subjected to monotonic and fatigue loadings at RT and 1000°C. Under both types of loading, the interlaminar pores appeared to have acted as the stress concentration sites, and matrix cracks initiated from these pores. Fig. 8 shows the crack initiation from an interlaminar pore, on the tensile surface of an edge-on specimen fatigue loaded at 1000°C in argon. In most of the samples subjected to monotonic or fatigue loadings, the specimen separation occurred along the interlaminar pores. The tensile surfaces of an edge-on specimen fatigue loaded to failure at RT are shown in Fig. 9. It is apparent from Fig. 9 that the specimen separation occurred along the interlaminar pores.

Although, the UFS values were significantly higher for the 0.006 m wide specimens of 0.050 m or 0.090 m in length, as compared to those for the 0.002 m wide samples of 0.050 m or 0.090 m in length tested in the edge-on or transverse orientations, there were no discernible changes in the specimen failure modes as the specimen length and/or width were increased. The specimen separation occurred along interlaminar pores in most of the specimens tested at RT and 1000°C.

Based on the metallographic observations of a large number of samples monotonically and cyclically loaded to failure, we propose the following sequence of fracture mechanisms in the Nicalon/SiC composite used in the present study (Fig. 10). Under monotonic and fatigue loadings, cracks initiate from the interlaminar pores and propagate primarily into the matrix. Final failure of the material, in both orientations, occurs when the matrix cracks link-up with the interlaminar pores, resulting in specimen severance along the interlaminar pores.

4.2. Specimen size effects on the UFS values

For the specimens with 0.002 m × 0.002 m cross-sections, the UFS values were unaffected by the loading span, in either edge-on or transverse orientations, at RT as well as 1000°C. Although a higher volume of the material was tested using the 0.090 m long specimens, as compared to the 0.050 m long samples, the failure modes were similar

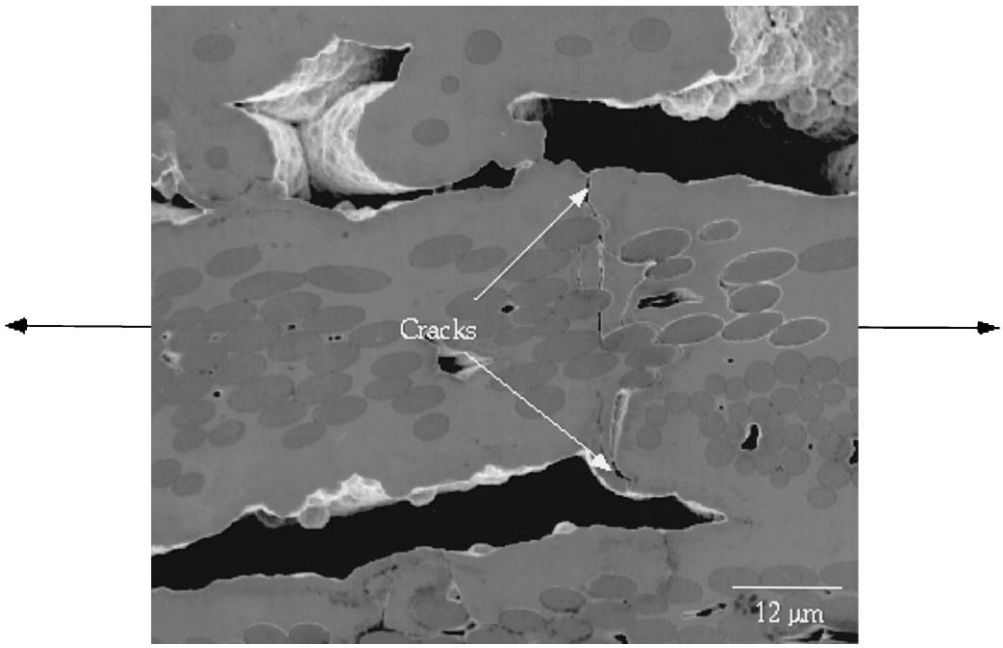

Fig. 8. Crack initiation from an interlaminar pore, on the tensile surface of a Nicalon/SiC edge-on specimen fatigue loaded at 1000°C in argon.

(in both cases the specimen severance occurred along the interlaminar pores), resulting in similar UFS values. When the specimen width was increased from 0.002 m to 0.006 m, however, there was a significant increase in the σ_{pl} and UFS values, which could be related to the fabric architecture. The 0.006 m wide specimens were tested only in the transverse orientation (the load was applied normal to the fabric plies). As noted elsewhere, porosity was present at the yarn intersections in the Nicalon/SiC composite used in the present study (Fig. 1). Mizuno et al. [19], who studied the tensile behavior of a plain-weave Nicalon/SiC, noticed that the pores at the yarn-intersection can act as stress concentration sites, and cracks can initiate from these pores. In the 0.002 m wide specimens used in the present study, on the average, there was only one intersection of the axial and braid-yarns. Thus, there was only one 'unit cell' of the fabric along the width direction of the tensile surface of a 0.002 m wide transverse specimen

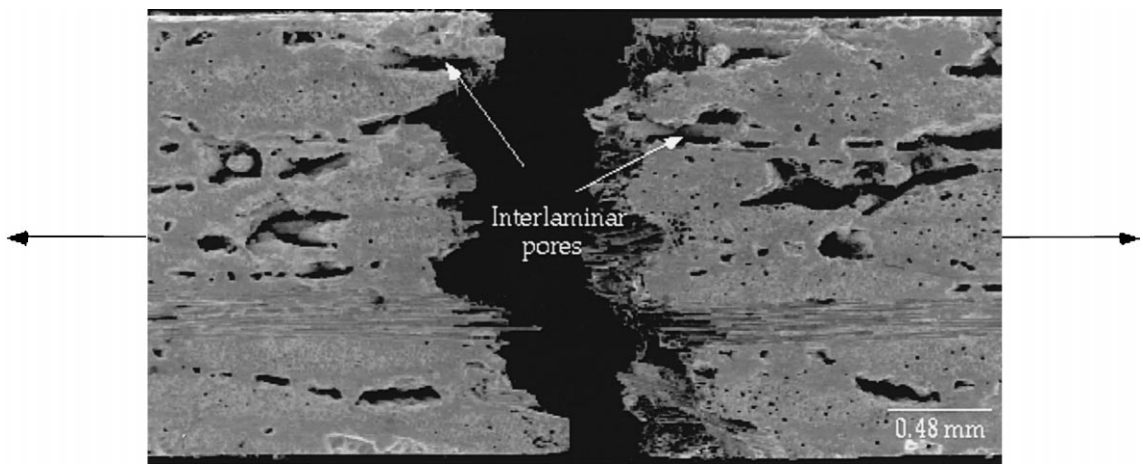

Fig. 9. Tensile surfaces of a Nicalon/SiC edge-on specimen fatigue loaded to failure at room temperature in air.

(Fig. 11). In such a specimen, it was relatively easy for any cracks initiated from the pores at the yarn intersection to propagate to the specimen edges uninterrupted. In a 0.006 m wide specimen, there were three 'unit cells' of the fabric on the tensile surface and, hence, there was a more efficient fiber-reinforcement of the matrix.

In a 0.006 m wide specimen, the cracks had to propagate through a much larger volume of the material to cause specimen failure than in a 0.002 m wide sample. Moreover, the crack path was more tortuous in a 0.006 m wide specimen, than in a 0.002 m specimen. In a 0.006 m wide specimen, the crack propagation direction could change

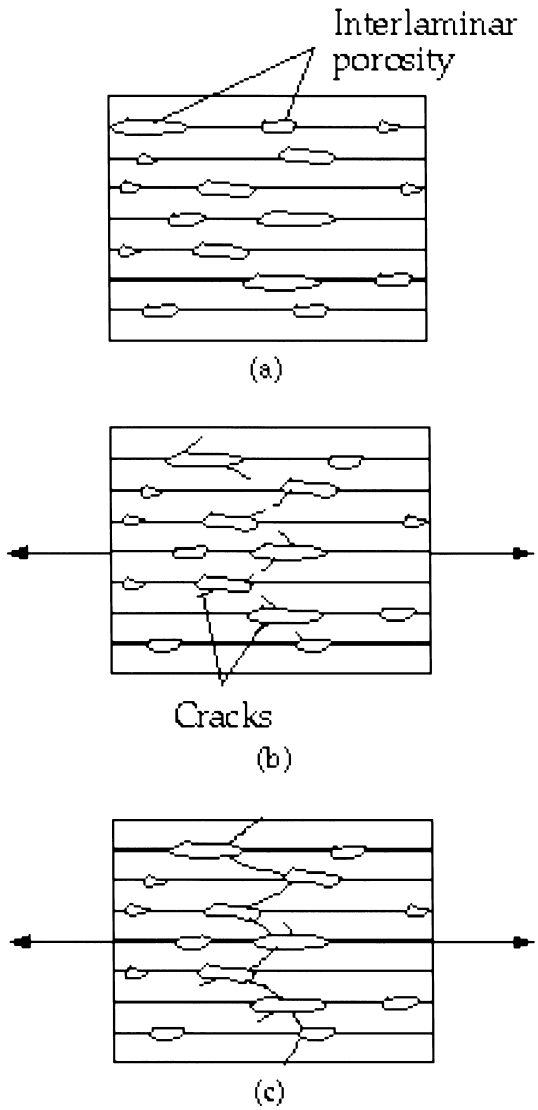

Fig. 10. Sequence of fracture mechanisms in the Nicalon/SiC composite under monotonic and fatigue loadings: (a) before loading, (b) crack initiation from the interlaminar pores and propagation into braid yarns, and (c) matrix crack linkup with the interlaminar pores, leading to specimen failure.

when a crack encountered yarns in the different (0°, +45° and −45°) directions, which was precluded in a 0.002 m wide specimen. Consequently, the σ_{pl} and UFS values were significantly higher for the 0.006 m specimens, as compared to those for the 0.002 m wide specimens tested in the transverse orientation, at both RT and 1000°C. This trend suggests that an objective assessment of the flexural behavior of fabric-reinforced composites should be made on specimens that are wide enough, such that multiple 'unit cells' of the fabric are present on the tensile surfaces.

Under flexure loading, laminate composites in the edge-on orientation are subjected to in-plane shear stress, while in the transverse orientation they experience interlaminar shear stress. Raghuraman et al. [20] showed that the UFS of a CFCC with low interlaminar shear strength increases as the ratio of the loading span to thickness is increased (owing to the increased probability of a tensile mode of failure) and approaches a constant value at high span-to-thickness ratios. In the present study, however, a change in the specimen length did not noticeably affect either the UFS values or the failure mechanisms in both edge-on and transverse orientations. This suggests that the in-plane and interlaminar shear strengths of the Nicalon/SiC composite are higher than the shear stress levels reached during the flexure testing of the 0.050 or 0.090 m long specimens. In addition, the identical failures modes in the edge-on and transverse orientations indicate that the laminae are strongly bonded to each other and the interlaminae boundaries are not weak layers.

In brittle materials, when the specimen size is increased, the UFS decreases due to the increased probability of the occurrence of strength limiting flaws. But, in the present investigation, the UFS values were unaffected by a change in the specimen length from 0.050 to 0.090 m in both edge-on and transverse orientations. However, at higher span-to-thickness ratios than those used in the present study, we believe that the UFS values in both edge-on and transverse orientations will be lower than those obtained in the current investigation.

4.3. Fatigue behavior

From the *S–N* data (Figs. 5 and 6) it appears that the fatigue limit was relatively high for the Nicalon/SiC composite in both edge-on and transverse orientations. The composite specimens survived 1 million load cycles at stress levels as high as 80% of the UFS values in both orientations, at room and elevated temperatures. Apparently, the prolonged exposure of the composite to 1000°C in an argon atmosphere did not noticeably degrade the fatigue life of the material.

The σ_{max} levels used during the fatigue tests were higher than the σ_{pl} values, at both RT and 1000°C. At stress levels higher than σ_{pl}, significant matrix cracking can occur on the tensile surface of a specimen during the first load cycle. Once fatigue-induced damage accumulates

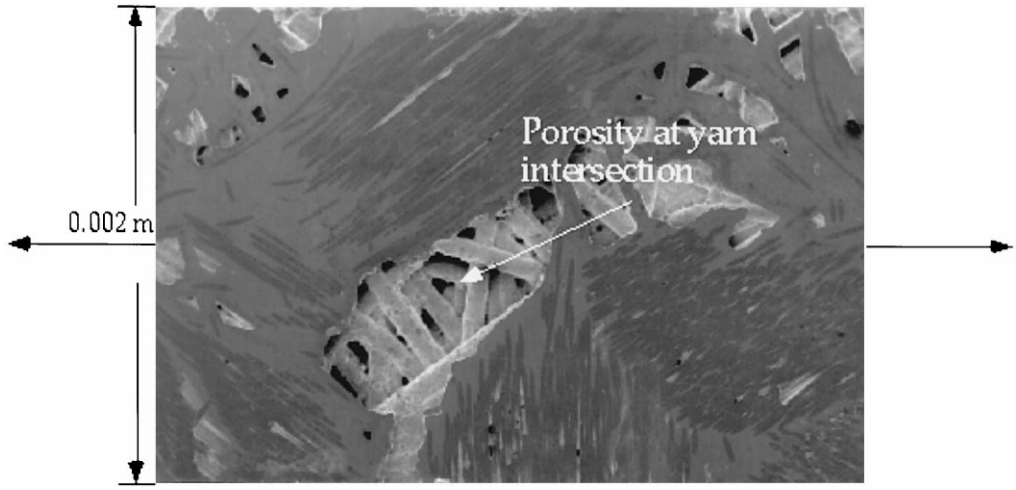

Fig. 11. Typical tensile surface of a 0.002 m wide Nicalon/SiC specimen in the transverse orientation.

on the tensile side of the specimens, the tensile surface loses the load bearing capacity. As a consequence, the neutral axis shifts to the compression side of the specimen, which alters the stress distribution in the specimen. Moreover, there can be a significant decrease in the interfacial shear strength due to repeated sliding at the fiber/matrix interface [19,21]. Thus, the σ_{max} values calculated using Eq. (1) are not strictly valid after the first load cycle. Therefore, the trends observed in the *S–N* behavior should be viewed as purely *qualitative*.

From the drop in the effective modulus values after the first cycle, during the fatigue tests at room and elevated temperatures, it was apparent that there was a significant degradation in the stiffness of the specimens due to cyclic loading. The initial drop in the modulus values (in the first 1000 load cycles) can be attributed to the propagation of the matrix microcracks, which initiate primarily from the interlaminar pores. The continued drop in the modulus values beyond 1000 load cycles may be attributed to the degradation in the interfacial shear strength due to repeated sliding at the fiber/matrix interface [19,21].

There can be an additional degradation of the interface, if the elevated-temperature tests are performed in air, rather than in an argon environment. In oxidizing atmospheres, the carbon interlayer may be removed by oxidation, resulting in the formation of a silica (SiO_2) film at the fiber/matrix interface [22,23]. If the silica bonds the fiber and the matrix together, a strong interfacial bonding may develop leading to catastrophic failure of the material. Hence, the *S–N* behavior of the composite may be significantly different from that observed in the present study, if the elevated-temperature fatigue tests are performed in air. However, if the oxidation of the interlayer is prevented by using oxide-based materials, such as mullite as the fiber-coatings [24,25], the Nicalon/SiC composites can be candidates for high-temperature structural applications. The oxidation of the Nicalon/SiC composites, with a carbon interface, may also be controlled by the efficient use of surface coatings, such as SiC, to prevent the access of oxygen to the fiber/matrix interface during the elevated-temperature exposure.

As indicated elsewhere, the effective modulus values were used in the present study to *qualitatively* estimate the progressive damage in the material during the fatigue tests. The effective modulus trends for the edge-on and transverse specimens fatigue tested at RT and 1000°C indicated that most of the stiffness degradation during the fatigue tests occurred in the first 10 cycles. Butkus et al. [26], Moschelle [27], Elahi et al. [28], and Unal [29–31] investigated the tensile fatigue behavior of Nicalon/SiC composites with different fabric-architectures, and reported that most of the reduction in the modulus of the material occurred in the first few cycles. Thus, it appears reasonable to use the effective modulus values to *at least qualitatively* study the progressive damage in CFCCs specimens subjected to flexure-fatigue loading.

Metallographic examination of the specimens subjected to cyclic loading revealed that matrix cracks initiated primarily from the interlaminar pores. Therefore, it is suggested that the interlaminar weakness of the Nicalon/SiC composite should be reduced by modifying the ICVI process to obtain the composite with reduced interlaminar porosity content. A reduced porosity content of the composite may also result in increased UFS and fatigue limit values.

5. Summary

(1) The fabric orientation did not noticeably influence the monotonic and fatigue behavior of a 2D braided Nicalon/SiC composite manufactured by an isothermal

chemical vapor infiltration (ICVI) process, either at RT in air or at 1000°C in an argon environment.

(2) The flexural stress–strain or fatigue (S–N) behavior of the Nicalon/SiC composite was not noticeably influenced by the test temperature. For a particular orientation, the flexural strength values were comparable at RT and 1000°C. Under fatigue loading, the samples survived one million load cycles at stress levels up to 80% of the flexural strength values, in both orientations, at room as well as elevated temperatures.

(3) The flexural strength values were unaffected by an increase in the loading span from 0.050 mm to 0.090 m, either at RT or 1000°C, in both edge-on and transverse orientations. However, a further increase in the loading span is expected to result in a reduction in the strength values.

(4) There was a significant increase in the flexural strength when the specimen width was changed from 0.002 m to 0.006 m, which was related to the fabric architecture. It was evident that the fabric architecture should be carefully considered when designing the test specimens so that multiple 'unit cells' of the fabric are subjected to the maximum loads during the tests, to objectively study the mechanical behavior of CFCCs.

(5) Under monotonic and fatigue loadings, the interlaminar pores in the material appeared to have acted as the stress concentration sites, and the cracks initiated from these pores. The link up of the matrix cracks with the interlaminar pores resulted in specimen severance under monotonic and fatigue loadings, in both edge-on and transverse orientations. Therefore, it appears that a decrease in the porosity content of the Nicalon/SiC, which may be achieved my refining the ICVI process, can result in increased flexural strength and fatigue limit values.

Acknowledgements

This research was supported by the Department of Energy under a contract from Lockheed Martin Energy Corporation (No. 11X-SV483V) to the University of Tennessee, and by a grant from the Southeastern University Research Association (SURA) to perform a 1996 Summer Cooperative Research Program in Materials Science at the Oak Ridge National Laboratory. One of the authors (P.K.L.) acknowledges the support from the National Science Foundation under Contract No. EEC-9527527 to the University of Tennessee, with M. Poats as the program manager. We are grateful to J. Armstrong of AlliedSignal Engines, for donating the composite material used in the present study. Many thanks are due to E.E. Bloom, A.F. Rowcliffe, A.M. Williams, J.W. Jones and D.W. Coffey of the Oak Ridge National Laboratory, T.E. Hutchinson of SURA, and T.A. Long, G.L. Jones and D.E. Fielden of The University of Tennessee for their help and support.

References

[1] G.R. Hopkins, J. Chin, J. Nucl. Mater. 148 (1986) 141.
[2] R.H. Jones, C.H. Henager Jr., G.W. Hollenberg, J. Nucl. Mater. 75 (1992) 191.
[3] L.L. Snead, doctoral thesis, Rensselaer Polytechnic Institute, 1992.
[4] N. Miriyala, P.K. Liaw, JOM 48 (9) (1996) 44.
[5] N. Miriyala, P.K. Liaw, JOM 4 (7) (1997) 59.
[6] A.S. Fareed, in: Handbook on Continuous Fiber-Reinforced Ceramic-Matrix Composites, R.L. Lehman, S.K. El-Rahaiby and J.B. Wachtman, Jr. (Eds.), Purdue University, West Lafayette, IN and The American Ceramic Society, Westerville, OH, 1995, p. 301.
[7] T.M. Besmann, B.W. Sheldon, R.A. Lowden, D.P. Stinton, Science 253 (1991) 1104.
[8] N. Miriyala, P.K. Liaw, C.J. McHargue, L.L. Snead, A.S. Fareed, Ceram. Trans. 74 (1996) 447.
[9] N. Miriyala, P.K. Liaw, C.J. McHargue, L.L. Snead, J.A. Morrison, Ceram. Eng. Sci. Proc. 18 (3) (1997) 747.
[10] N. Miriyala, doctoral dissertation, The University of Tennessee at Knoxville, 1997.
[11] ASTM Designation C 1341, Annual Book of ASTM Standards, American Society for Testing and Materials, Philadelphia, PA, 1997.
[12] C.A. Folsom, F.W. Zok, F.F. Lange, J. Am. Ceram. Soc. 77 (1994) 689.
[13] P.S. Steif, A. Trojnacki, J. Am. Ceram. Soc. 77 (1994) 221.
[14] W.A. Curtin, J. Am. Ceram. Soc. 74 (1991) 2837.
[15] W.A. Curtin, J. Am. Ceram. Soc. 77 (1994) 1072.
[16] W.A. Curtin, J. Am. Ceram. Soc. 77 (1994) 1075.
[17] J.J. Kibler, S.G. DiPietro, Ceram. Eng. Sci. Proc. 16 (5) (1995) 809.
[18] P.K. Liaw, D.K. Hsu, N. Yu, N. Miriyala, V. Saini, H. Jeong, Acta Metall. Mater. 44 (1996) 2101.
[19] M. Mizuno, S. Zhu, Y. Nagano, Y. Sakaida, Y. Kagawa, M. Watanabe, J. Am. Ceram. Soc. 79 (1996) 3065.
[20] S. Raghuraman, E. Lara-Curzio, M.K. Ferber, Ceram. Eng. Sci. Proc. 17 (4) (1996) 147.
[21] A.G. Evans, F.W. Zok, R.M. McMeeking, Acta Metall. Mater. 43 (1995) 859.
[22] P.F. Tortorelli, S. Nijhawan, L. Riester, R.A. Lowden, Ceram. Eng. Sci. Proc. 14 (7&8) (1993) 358.
[23] R.H. Jones, C.H. Henager, P.F. Tortorelli, JOM 45 (1993) 26.
[24] S. Shanmugham, D.P. Stinton, F. Rebillat, A. Bleier, T.M. Besman, Ceram. Eng. Sci. Proc. 16 (4) (1995) 389.
[25] S. Shanmugham, P.K. Liaw, D.P. Stinton, T.M. Besmann, K.L. More, A. Bleier, W.D. Porter, S.T. Misture, Ceram. Trans. 79 (1996) 71.
[26] L.M. Butkus, L.P. Zawada and G.A. Hartman, Room temperature tensile and fatigue properties of silicon–carbide fiber-reinforced ceramic matrix composites, Paper presented at Aeromet'90, Long Beach, California, May 1990.
[27] W.R. Moschelle, Ceram. Eng. Sci. Proc. 15 (4) (1994) 13.
[28] M. Elahi, K. Reifsnider, T. Dunyak, K. Liao, Ceram. Eng. Sci. Proc. 17 (4) (1996) 357.
[29] O. Unal, Ceram. Eng. Sci. Proc. 17 (4) (1996) 157.
[30] O. Unal, Ceram. Trans. 74 (1996) 435.
[31] O. Unal, J. Mater. Sci. Lett. 15 (1996) 789.